

## OBSERVATIONAL EVIDENCE OF GENTLE CHROMOSPHERIC EVAPORATION DURING THE IMPULSIVE PHASE OF A SOLAR FLARE

RYAN O. MILLIGAN,<sup>1,2</sup> PETER T. GALLAGHER,<sup>2,3,4</sup> MIHALIS MATHIOUDAKIS,<sup>1</sup> AND FRANCIS P. KEENAN<sup>1</sup>

Received 2006 March 13; accepted 2006 March 27; published 2006 April 14

### ABSTRACT

Observational evidence of gentle chromospheric evaporation during the impulsive phase of a C9.1 solar flare is presented using data from the *Reuven Ramaty High-Energy Solar Spectroscopic Imager* and the Coronal Diagnostic Spectrometer on board the *Solar and Heliospheric Observatory*. Until now, evidence of gentle evaporation has often been reported during the decay phase of solar flares, where thermal conduction is thought to be the driving mechanism. Here we show that the chromospheric response to a low flux of nonthermal electrons ( $\geq 5 \times 10^9$  ergs cm<sup>-2</sup> s<sup>-1</sup>) results in plasma upflows of  $13 \pm 16$ ,  $16 \pm 18$ , and  $110 \pm 58$  km s<sup>-1</sup> in the cool He I and O V emission lines and the 8 MK Fe XIX line, respectively. These findings, in conjunction with other recently reported work, now confirm that the dynamic response of the solar atmosphere is sensitively dependent on the flux of incident electrons.

*Subject headings:* Sun: atmospheric motions — Sun: flares — Sun: UV radiation — Sun: X-rays, gamma rays

*Online material:* color figure

### 1. INTRODUCTION

During the impulsive phase of a solar flare, accelerated electrons propagate along closed magnetic field lines to the dense, underlying chromosphere, where they lose their energy via Coulomb collisions and heat the local plasma. The resulting expansion of this plasma is known as “chromospheric evaporation.” From the hydrodynamic simulations of Fisher et al. (1985a, 1985b, 1985c) and, more recently, Abbett & Hawley (1999), the solar atmosphere is predicted to respond in one of two ways, depending on the flux of accelerated nonthermal electrons.

For electron fluxes  $\leq 10^{10}$  ergs cm<sup>-2</sup> s<sup>-1</sup>, the evaporated plasma flows upward at several tens of kilometers per second, with no associated downflows. This process is termed “gentle” evaporation. Gentle evaporation may also occur during the decay phase, when the upflows are driven by thermal conduction rather than electron beam heating (Antiochos & Sturrock 1978). Many studies have reported evidence of conduction-driven evaporation during the decay phase of solar flares (Schmieder et al. 1987; Zarro & Lemen 1988; Czaykowska et al. 2001; Berlicki et al. 2005). In each of these studies it was concluded that the late-phase evaporation was caused by heat conduction along field lines connecting the chromosphere to the corona. Evidence of gentle evaporation was also presented by Brosius & Phillips (2004) during flare precursor events and by Singh et al. (2005) during coronal loop formation, but in these cases the mechanism(s) responsible could not be verified. To date, there has been no direct evidence of gentle evaporation due to nonthermal electrons during the impulsive phase of a solar flare.

At high nonthermal electron fluxes ( $\geq 3 \times 10^{10}$  ergs cm<sup>-2</sup> s<sup>-1</sup>), the chromosphere is unable to radiate at a sufficient rate and consequently expands rapidly. The heated chromospheric plasma ( $\sim 10^7$  K) expands upward at hundreds of kilometers per second in a process known as “explosive” evaporation. The overpressure of the flare plasma relative to the underlying chromosphere also

causes cooler, more dense material to expand downward at tens of kilometers per second. This process is known as “chromospheric condensation.” A strong case for explosive evaporation was presented by Brosius & Phillips (2004), who reported oppositely directed flows using the Coronal Diagnostic Spectrometer (CDS; Harrison et al. 1995) on board the *Solar and Heliospheric Observatory (SOHO)* during a hard X-ray (HXR) burst. A more recent study by Milligan et al. (2006, hereafter Paper I) also found these flows patterns, but, critically, they were able to derive the properties of the driving electron beam using simultaneous HXR imaging and spectroscopy from the *Reuven Ramaty High-Energy Solar Spectroscopic Imager (RHESSI)*; Lin et al. 2002).

In this Letter we present the first observational evidence of gentle chromospheric evaporation due to nonthermal electrons during the impulsive phase of a solar flare. A brief overview of the instruments and data analysis is given in § 2 (a more detailed description can be found in Paper I). Our results are then presented in § 3, while a discussion and conclusions are given in § 4.

### 2. OBSERVATIONS

Our study focuses on a compact *GOES* C9.1 flare, which began at 11:40:08 UT on 2002 July 15. The flare occurred close to the solar meridian ( $-40''$ ,  $232''$ ) during a joint observing plan between *RHESSI* and other ground- and space-based observatories. Unfortunately, there were no complimentary EUV images available from either the EUV Imaging Telescope (EIT) or the *Transition Region and Coronal Explorer* during the event.

The CDS observations reported here were acquired with the FLARE\_AR observing sequence (see Paper I for details). Images taken during the impulsive phase in the He I (584.33 Å), O V (629.73 Å), and Fe XIX (592.23 Å) emission lines are shown in Figure 1. Spectra from each CDS pixel were fitted with a broadened Gaussian profile (Thompson 1999), for each of the spectral windows. Velocities were found by measuring Doppler shifts relative to quiet-Sun spectra, which were assumed to be emitted by stationary plasma. A heliographic correction was also applied assuming purely radial flows.

*RHESSI* is an imaging spectrometer capable of observing X-

<sup>1</sup> Department of Physics and Astronomy, Queen’s University Belfast, Belfast BT7 1NN, Northern Ireland.

<sup>2</sup> Laboratory for Solar and Space Physics, NASA Goddard Space Flight Center, Greenbelt, MD 20771.

<sup>3</sup> School of Physics, Trinity College Dublin, Dublin 2, Ireland.

<sup>4</sup> L-3 Communications GSI.

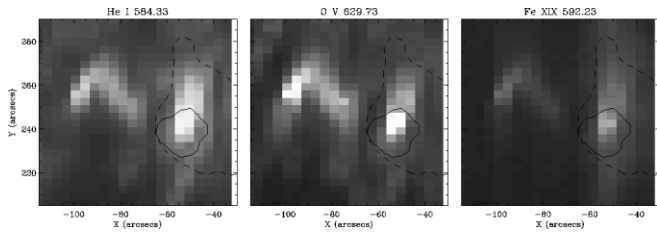


FIG. 1.—CDS images obtained in the He I ( $\log T = 4.5$ ), O V ( $\log T = 5.4$ ), and Fe XIX ( $\log T = 6.9$ ) emission lines observed during the impulsive phase of the 2002 July 15 solar flare. *RHESSI* 6–16 keV (dotted line) and 16–50 keV (solid lines) contours are overlaid, drawn at 5% and 10% of the peak intensity, respectively. [See the electronic edition of the *Journal* for a color version of this figure.]

ray and  $\gamma$ -ray emission over a wide range of energies ( $\sim 3$  keV–17 MeV). The thin attenuators on *RHESSI* were in place during part of the impulsive phase of this event, thus limiting the energy range to  $\geq 6$  keV. Flare emission was not observed above  $\sim 50$  keV. The observing summary data for the energy ranges 6–12, 12–25, and 25–50 keV are shown in the top panel of Figure 2. As *RHESSI* went into eclipse at  $\sim 11:49:00$  UT, the *GOES* light curve for this event was overplotted for completeness. During this time, the 25–50 keV emission returned to its nonsolar background level. Both the *RHESSI* images and spectra were formed over a 76 s period from 11:43:36 to 11:44:52 UT to coincide with the time range over which CDS observed blueshifts in the Fe XIX line. This time interval is indicated by two vertical dotted lines in the top panel of Figure 2 and includes the impulsive 25–50 keV HXR burst. *RHESSI* images in two energy bands (6–16 and 16–50 keV) were reconstructed using the Pixion algorithm (Hurford et al. 2002). Contours at 5% and 10% of the peak intensity, respectively, in each band are overlaid on each EUV image in Figure 1. The *RHESSI* spectrum was fitted assuming an isothermal distribution at low energies and thick-target emission at higher energies (bottom panel of Fig. 2).

### 3. RESULTS

The thick-target model solution, consistent with the *RHESSI* photon spectrum, produced an electron distribution with a low-energy cutoff ( $\epsilon_c$ ) of  $\sim 20$  keV and a power-law index ( $\delta$ ) of  $\sim 5.2$ ; a break energy of  $\sim 20$  keV in the electron spectrum corresponds to a break energy of  $\sim 16$  keV in the associated photon spectrum. From the properties of the inferred electron spectrum, the total power of nonthermal electrons was found

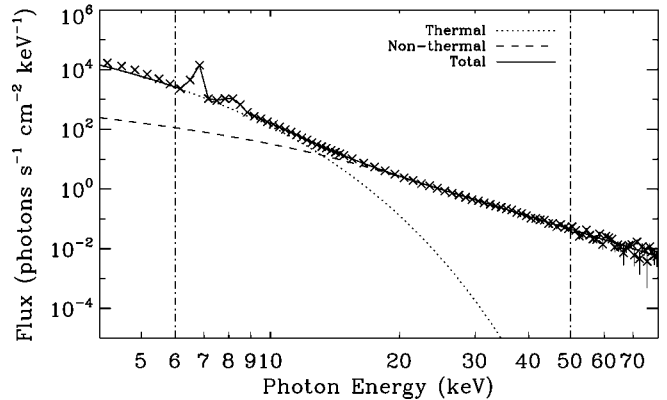
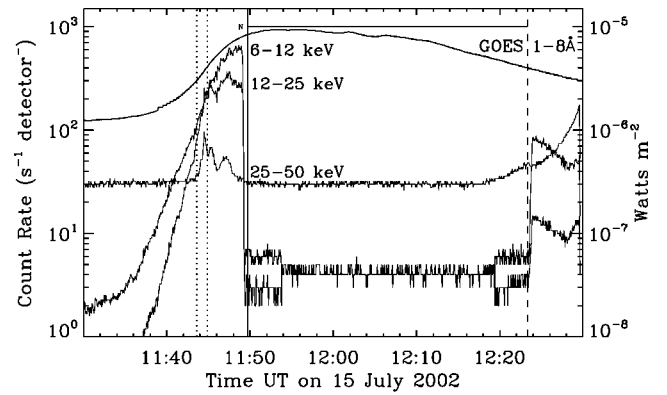


FIG. 2.—*Top panel*: *RHESSI* observing summary data (corrected for changes in attenuator states) from the 6–12, 12–25, and 25–50 keV bands. The vertical dotted lines indicate the time interval over which images and spectra were formed, corresponding to the observation of significant upflows with CDS. The bar denoted “N” at the top of the plot illustrates the period that *RHESSI* was in eclipse. Overplotted is the *GOES* 1–8 Å curve. *Bottom panel*: Portion of the *RHESSI* spectrum integrated over the time range given above. The energy range 6–50 keV lying between the vertical dot-dashed lines was fitted assuming an isothermal component (dotted curve) and a thick-target bremsstrahlung component (dashed curve).

to be  $\sim 8 \times 10^{27}$  ergs  $s^{-1}$ . The reconstructed 16–50 keV image yielded an upper limit to the HXR source size of  $\sim 1.8 \times 10^{18}$  cm $^2$ , and the resulting flux of nonthermal electrons was therefore found to be  $\geq 5 \times 10^9$  ergs cm $^{-2}$   $s^{-1}$ .

Figure 3 shows the spatial distribution of the plasma flows seen in each of the He I, O V, and Fe XIX lines. Net upflows of  $13 \pm 16$  and  $16 \pm 18$  km  $s^{-1}$  were observed in the He I

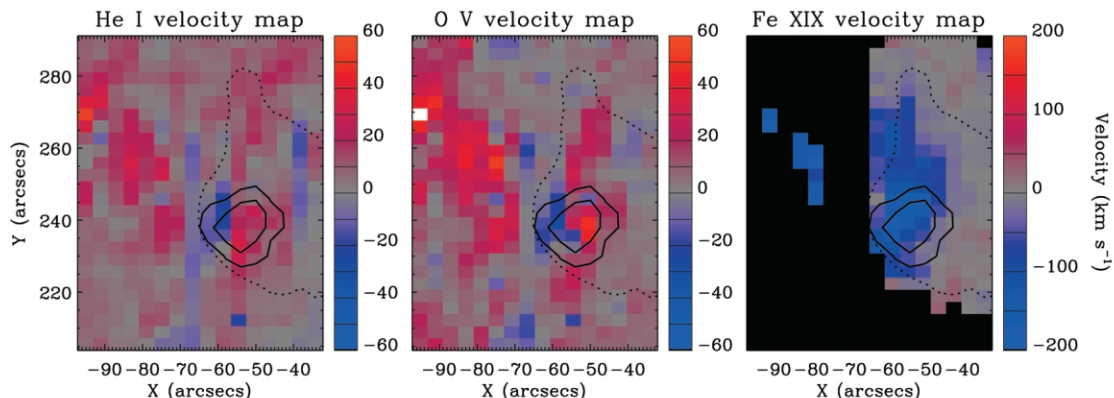


FIG. 3.—Velocity maps in the He I, O V, and Fe XIX lines. Downflows are indicated by red pixels, while upflows are given in blue pixels. The solid contours denote the *RHESSI* 16–50 keV emission at 10% and 50% of the peak intensity, while the dotted contour shows the 6–16 keV emission at 5% of the peak intensity.

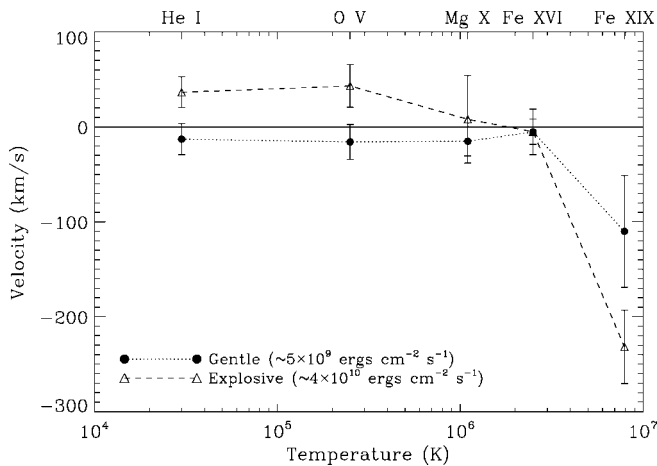


FIG. 4.—Plasma velocity as a function of temperature for each of the five lines observed using CDS. Positive velocities indicate downflows, while negative values indicate upflows. The data points plotted with filled circles denote the values presented in this study, while the open triangles illustrate those values presented in Paper I for the case of explosive evaporation. The dotted and dashed lines connecting the points are added to guide the reader.

and O v maps, respectively, by averaging over all CDS pixels within the 16–50 keV 10% contour as observed by *RHESSI*. Moderately strong upflows of  $110 \pm 58 \text{ km s}^{-1}$  were observed in the Fe XIX map by averaging over the same area. Weaker flows of  $\leq 50 \text{ km s}^{-1}$  were measured away from this area and appear to be aligned with the thermal (6–16 keV) emission observed by *RHESSI*. The mean velocity (from within the HXR emitting area) as a function of temperature for each of the five emission lines observed by CDS is shown in Figure 4. No significant flows were measured in either the Mg x or Fe XVI lines, which would appear to be characteristic of plasma at 1–2 MK (see also Singh et al. 2005 and Paper I). Error bars represent a  $1 \sigma$  uncertainty. The values reported in Paper I for the case of explosive evaporation (electron flux  $\geq 4 \times 10^{10} \text{ ergs cm}^{-2} \text{ s}^{-1}$ ) are overplotted.

#### 4. DISCUSSION AND CONCLUSIONS

Simultaneous X-ray and EUV observations of gentle chromospheric evaporation during the impulsive phase of a C9.1 solar flare are presented using data from *RHESSI* and *SOHO*/CDS. Until now, studies that reported evidence of gentle evaporation were entirely focused on low-velocity ( $\leq 80 \text{ km s}^{-1}$ ) mass motions observed during the decay phase of solar flares (Schmieder et al. 1987; Zarro & Lemen 1988; Czaykowska et al. 2001; Berlicki et al. 2005). In each of these cases, the mechanism responsible was believed to be thermal conduction caused

by the steep temperature gradients between the high-temperature flare plasma and the cool, underlying chromosphere (Antiochos & Sturrock 1978). This was also motivated by the fact that power-law spectra are not observed during the decay phase of the majority of solar flares.

In this Letter, we report the first observational evidence of gentle evaporation due to nonthermal electrons during the impulsive phase of a solar flare as predicted by current theoretical models. Upflows of  $13 \pm 16$ ,  $16 \pm 17$ , and  $110 \pm 58 \text{ km s}^{-1}$  as seen in the He I, O v, and Fe XIX lines, respectively, result from a beam of nonthermal electrons with a flux value of  $\geq 5 \times 10^9 \text{ ergs cm}^{-2} \text{ s}^{-1}$ . From Paper I, we reported that an order of magnitude higher flux ( $\geq 4 \times 10^{10} \text{ ergs cm}^{-2} \text{ s}^{-1}$ ) gives rise to downflows of  $\sim 35$  and  $\sim 45 \text{ km s}^{-1}$  in the He I and O v lines, respectively, and upflows of  $\sim 270 \text{ km s}^{-1}$  in the Fe XIX line. As a consequence, the findings reported here and in Paper I support the theoretical models predicting that the response of the solar chromosphere is sensitively dependent on the flux of accelerated nonthermal electrons. Our results also support the prediction that there exists a threshold value for the nonthermal electron flux above which the chromosphere cannot efficiently radiate the deposited energy. Fisher et al. (1985a) proposed that this threshold value is  $\sim 3 \times 10^{10} \text{ ergs cm}^{-2} \text{ s}^{-1}$ . Above this value, electron fluxes were shown to begin to drive chromospheric condensation, a process resulting from the high pressures reached by the rapidly expanding evaporated material. The combination of the results presented here and in Paper I also lends very strong evidence to support this principle.

The recent hydrodynamic simulations of Abbett & Hawley (1999) and Allred et al. (2005) have been developed to include more realistic electron-beam parameters and a non-LTE treatment of the solar atmosphere. These more detailed calculations still provide the distinction between gentle and explosive evaporation for differing nonthermal electron fluxes. These models will be further developed to include higher temperature plasmas that will be observed by the EUV Imaging Spectrometer (EIS) on board *Solar-B*, due for launch in late 2006. By combining EIS observations with *RHESSI* data in the future, an even greater understanding of the behavior of high-temperature plasmas during solar flares will be achieved.

This work has been supported by a Department of Employment and Learning studentship in conjunction with a Cooperative Award in Science and Technology from NASA Goddard Space Flight Center. F. P. K. is grateful to A. W. E. Aldermaston for the award of a William Penny Fellowship. We would like to thank Brian Dennis and the *RHESSI* team, Joe Gurman, and Dominic Zarro at Goddard for their continued support. *SOHO* is project of international collaboration between the European Space Agency and NASA.

#### REFERENCES

- Abbett, W. P., & Hawley, S. L. 1999, *ApJ*, 521, 906  
 Allred, J. C., Hawley, S. L., Abbett, W. P., & Carlsson, M. 2005, *ApJ*, 630, 573  
 Antiochos, S. K., & Sturrock, P. A. 1978, *ApJ*, 220, 1137  
 Berlicki, A., Heinzel, P., Schmieder, B., Mein, P., & Mein, N. 2005, *A&A*, 430, 679  
 Brosius, J. W., & Phillips, K. J. H. 2004, *ApJ*, 613, 580  
 Czaykowska, A., Alexander, D., & De Pontieu, B. 2001, *ApJ*, 552, 849  
 Fisher, G. H., Canfield, R. C., & McClymont, A. N. 1985a, *ApJ*, 289, 414  
 ———. 1985b, *ApJ*, 289, 425  
 ———. 1985c, *ApJ*, 289, 434  
 Harrison, R. A., et al. 1995, *Sol. Phys.*, 162, 233  
 Hurford, G. J., et al. 2002, *Sol. Phys.*, 210, 61  
 Lin, R. P., et al. 2002, *Sol. Phys.*, 210, 3  
 Milligan, R. O., Gallagher, P. T., Mathioudakis, M., Bloomfield, D. S., Keenan, F. P., & Schwartz, R. A. 2006, *ApJ*, 638, L117 (Paper I)  
 Schmieder, B., Forbes, T. G., Malherbe, J. M., & Machado, M. E. 1987, *ApJ*, 317, 956  
 Singh, J., Sakurai, T., Ichimoto, K., Suzuki, I., & Hagino, M. 2005, *Sol. Phys.*, 226, 201  
 Thompson, W. T. 1999, Post-Recovery Broadened Line Profiles (CDS Software Note 53; Chilton: Rutherford Appleton Lab.)  
 Zarro, D. M., & Lemen, J. R. 1988, *ApJ*, 329, 456